ISSN 2250-3153

Protons Confirmation of Glimepiride drug using Correlation Spectroscopy a unique tool of Nuclear Magnetic Resonance spectroscopy

*** Kartikeya Dwivedi ** Nitin Saraswat *** Meena Bisht**

* Maharaj Singh College ; Saharanpur (U.P)
** K.M.Institute of Pharmaceutical Sciences, Rourkela, Orissa
*** Kumaun University; Nainital;Bhimtaal Campus; Bhimtaal; Uttarakhand

***Abstract*:** The power of Nuclear Magnetic Resonance spectroscopy (NMR) in structure elucidation derives in large part from its ability to establish bonding connectivity (via J- coupling interaction) or through space proximity (via dipolar coupling interactions) of nuclei. The amount of time consumed in elucidating a structure depends on the rate at which these interaction can be detected by NMR and analyzed.1D NMR methods most often explore interactions between only few nuclei at a time: spin-spin decoupling measurements are used to demonstrate through-bond connectivity; and NOE measurements are used to probe inter-nuclear distances, 2-Dimensional NMR experiments provide much more structural information in a given time period. Correlation spectroscopy was used to elucidate the aromatic proton position in NMR spectra.

***Index Terms*:** NMR, J-coupling, dipolar coupling, NOE, 2 dimensional NMR

I. INTRODUCTION

a) Introduction to Glimepiride:

Glimepride is a medium- to long-acting sulfonylurea antidiabetic drug. It is sometimes classified as either the first third-generation sulfonylurea, or as second-generation. Glimepiride is indicated to treat type 2 diabetes mellitus; its mode of action is to increase insulin production by the pancreas. It is not used for type 1diabetes because the pancreas is no longer able to produce insulin.Its use is contraindicated in patients with hypersensitivity to glimepiride or other sulfonylureas, and during pregnancy. Side effects from taking glimepiride include gastrointestinal tract (GI) disturbance, and rarely thrombocytopenia, leukopenia, hemolytic anemia, and occasionally allergic reactions occur. In the initial weeks of treatment, the risk of hypoglycemia may be increased. Alcohol consumption and exposure to sunlight should be restricted in patients taking it because they can worsen the side effects. With glimepiride, GI absorption is complete, with no interference of meals. Significant absorption was seen within 1 hour, and distributed throughout the body, bound to the plasma protein to an extent of
99.5%. It is metabolized by oxidative biotransformation, and 60% is excreted in the urine, the
remaining being excreted in the feces. Like all sulfonylureas, glimepiride acts as an insulin secretagogue. It lowers blood sugar by stimulating the release of insulin by pancreatic
beta cells and by inducing increased activity of intracellular insulin receptors.Not all secondary sufonylureas have the same risks of hypoglycemia. Glimepiride likely binds to ATP sensitive potassium channel receptors on the pancreatic cell surface, reducing potassium conductance and causing depolarization of the membrane. Membrane depolarization stimulates calcium ion influx through voltage sensitive calcium channels, this increase in intracellular calcium ion concentration induces the secretion of insulin.

b) Introduction to Correlation Spectroscopy:

The key point in all this is that magnetisation transfer occurs between coupled spins. To appreciate the outcome of this in the final COSY spectrum, consider the case of
two J-coupled spins, A and X, with a coupling constant of J_{AX} and chemical shift offsets of $\surd_A$ and $\surd_x$. The magnetisation associated with spin A will, after the initial 90^0pulse, precess during t1 according to its chemical shift offset, $\surd_A$. The second 90^0 pulse then transfers some part of this magnetisation to the coupled X spin, whilst some remains associated with the original spin A. That which remains with A will then precess in the detection period at a frequency $\surd$A just as it did during t1, so in the final spectrum, will produce a peak at $\surd_A$ in both dimensions, denoted ($\surd_A$, $\surd_A$). This peak is therefore equivalent to that observed for the uncoupled AX system and because it represents the same frequency in both dimensions, it sits on the diagonal of the 2D spectrum and is therefore referred to as a diagonal peak. In contrast, the transferred magnetisation will precess in t_2 at the frequency of the new 'host' spin X and will thus produce a peak corresponding to two different chemical shifts in the two dimensions ($\surd_A$, $\surd_X$). This peak sits away from the diagonal and is therefore referred to as an off-diagonal or, more commonly, a crosspeak This is the peak of interest as it provides

direct evidence of coupling between spins A and X. The whole process operates in the reverse direction also, that is, the same arguments apply for magnetisation originally associated with the X spin, giving rise to a diagonal peak at ($\sqrt{}_x$, $\sqrt{}_x$) and a crosspeak at ($\sqrt{}_x$, $\sqrt{}_A$). Thus, the COSY spectrum is symmetrical about the diagonal, with crosspeaks on either side of it mapping the same interaction.

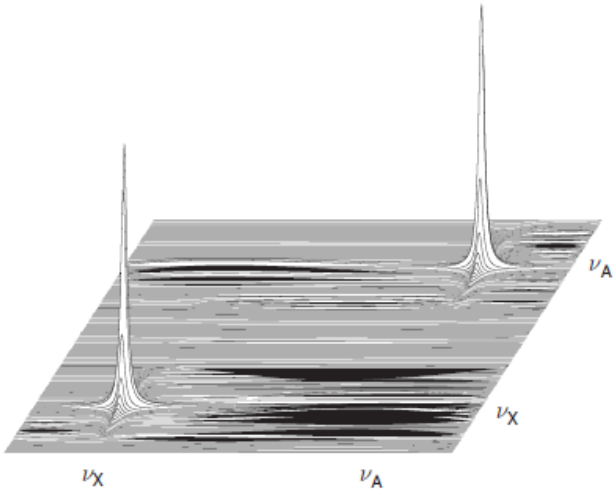

Figure-1: Sample containing two uncoupled spins, A and X, of offsets $\sqrt{}_A$ and $\sqrt{}_X$. Each produces a 2D peak at its corresponding chemical shift offset in both dimensions.

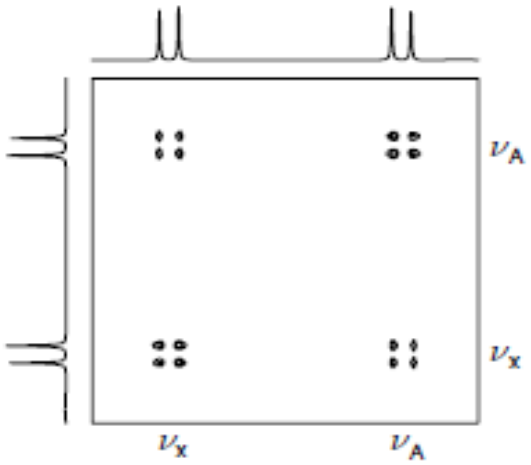

Figure-2 : The COSY spectrum of a coupled, two-spin AX system. Diagonal peaks are equivalent to those observed in the 1D spectrum whilst crosspeaks provide evidence of a coupling between the correlated spins.

Theory of polarisation transfer in the INEPT experiment, it was shown that the basic requirement for the transfer of polarization was an anti-phase disposition of the doublet vectors of the source spin, which for INEPT was generated by a spin-echo sequence. Magnetisation components that were in-phase just before the second 90^0 pulse would not contribute to the transfer, hence the Δ period was optimised to maximise the anti-phase component. The same condition applies for magnetisation transfer between two protons as in the COSY experiment. This requires that the proton–proton coupling be allowed to evolve to give a degree of anti-phase magnetisation that may be transferred by the second pulse, whilst the in-phase component remains associated with the original spin. The coupling evolution period for COSY is the t_1 period so that the amount of transferred magnetisation detected in t_2 is also modulated as a function of t_1 (sin $180Jt_1$). Likewise, the amplitude of the in-phase, non-transferred component is also modulated in t_1 by the coupling (cos $180Jt_1$), and this produces the coupling fine structure of the diagonal peak in f_1.

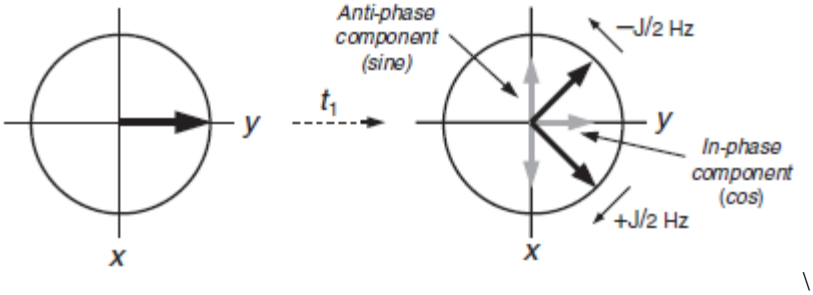

Figure-3: Coupling evolution during t_1 produces in-phase and antiphase magnetisation components. Only the anti-phase component contributes to magnetisation transfer and hence to crosspeaks in the 2D spectrum.

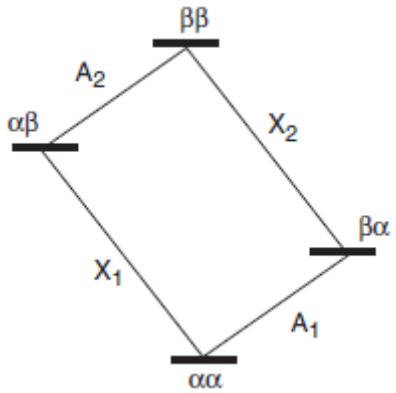

Figure-4: Schematic energy level diagrams for the coupled two spin AX system.

As for 1D data, f_1 quadrature detection requires two data sets that differ in phase by 90^0 to be collected, thus providing the necessary sine and cosine amplitude-modulated data. Since the f_1 dimension is generated artificially, there is strictly no reference rf to define signal phases, so it is the phase of the pulses that bracket t_1 that dictate the phase of the detected signal. Thus, for each t_1 increment, two data sets are collected, one with a 90_x preparation pulse (t_1 sine modulation) and the other with 90_y (t_1 cosine modulation), both stored separately These two sets are then equivalent to the two channel data collected with simultaneous acquisition, which produces the desired frequency discrimination when subject to a complex FT (also referred to as a hypercomplex transform in relation to 2D data). The rate of sampling in t_1 or, in other words, the size of the t_1 time increment, is dictated by the f_1 spectral width and is subject to the same rules as for the simultaneous sampling of one-dimensional data. This method is derived from the original work of States, Haberkorn and Ruben and is therefore often referred to in the literature as the States method of f_1 quad detection.

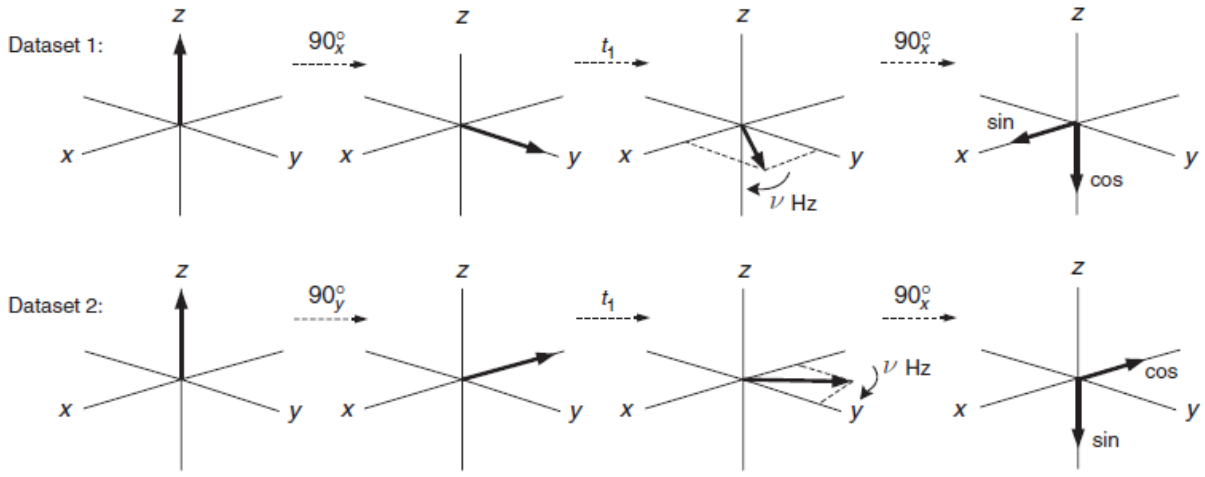

Figure-5: The States method of f_1 quadrature detection requires two data sets to be acquired per increment to generate separate sine- and cosine modulated data sets.

II. METHODOLOGY

The success of any NMR experiment is, of course, crucially dependent on the correct setting of the acquisition parameters. In the case of 2D experiments, one has to consider the parameters for each dimension separately, and we shall see that the most appropriate parameter settings for f_2 are rarely optimum for f1. Likewise, one has to give rather more thought to the setting up of a 2D experiment than is usually required for 1D acquisition to make optimum use of the instrument time available and data storage space. spectral widths, which should be the same in both dimensions of the COSY experiment, should be kept to minimum values with transmitter offsets adjusted so as to retain only the regions of the spectrum that will provide useful correlations. It is usually possible to reduce spectral widths to well below the 10-ppm or so proton window observed in 1D experiment. The use of excessively large windows leads to poorer digital resolution in the final spectrum or requires greater data sizes, neither of which is desirable. The spectral widths in turn define the sampling rates for data in t_2, in exact analogy with 1D acquisition, and the size of the t_1 increment, again according to the Nyquist criteria. The acquisition time (AQ_t), and hence the digital resolution ($1/AQ_t$), for each dimension is then dictated by the number of data points collected in each. For t_2, this is the number of data points digitised in each FID, whilst for t_1 this is the number of FIDs collected over the course of the experiment. The appropriate setting of these parameters is a most important aspect to setting up a 2D experiment, and the way in which one thinks about acquisition times and digital resolution in a 2D data set is, necessarily, quite different from that in a 1D experiment. As an illustration, imagine transferring the typical parameters used in a 1D proton acquisition into the two dimensions of COSY. The acquisition time might be 4 s, corresponding to a digital resolution of 0.25 Hz/pt, with no relaxation delay between scans. On, for example, a 400-MHz instrument, with a 10 ppm spectral width, this digital resolution would require 32K words to be collected per FID. The 2D equivalent, with States quad detection in f_1 and with axial-peak suppression, requires four scans to be collected for each t_1 increment. The mean acquisition time for each would be 6 s (t_2 plus the mean t_1 value), corresponding to 24 s of data collection per FID. If 16K t_1 increments were to be made for the f_1 dimension (two data sets are collected for each t_1 increment remember), this would correspond to a total experiment time of about 4.5 days. Furthermore, the size of the resulting data matrix would be a little over 1000 million words, and with a typical 32-bit-per-word computer system, this requires some 4GB of disk space! We will agree that 4 days for a basic COSY acquisition is quite unacceptable, let alone the need for such disk space per experiment; so acquiring data with such high levels of digitisation in both dimensions is clearly not possible.

The key lies in deciding on what level of digitisation is required for the experiment in hand. The first point to notice is that adding data points to extend the t_2 dimension leads to a relatively small increase in the overall length of the experiment, so we may be quite profligate with these (although they will lead to a corresponding increase in the size of the data matrix). Moreover, adding t1 data points requires that a complete FID of potentially many scans is required per increment, which makes a far greater increase to the total data collection time. Thus, one generally aims to keep the number of t_1 increments to a minimum, which is consistent with resolving the correlations of interest and increasing t_2 as required when higher resolution is necessary. For this reason, the digital resolution in f_2 is often greater than that in f_1, particularly in the case of phase-sensitive data sets. The use of smaller AQt_1 is, in general, also preferred for reasons of sensitivity since FIDs recorded for longer values of t_1 will be attenuated by relaxation and so will contribute less to the overall signal intensity. The use of small AQt_1 is likely to lead to truncation of the t_1 data, and it is then necessary to apply suitable window functions that force the end of the data to zero to reduce the appearance of truncation artefacts.

For COSY in particular, one of the factors that limits the level of digitisation that can be used is the presence of intrinsically anti-phase crosspeaks, since too low a digitisation will cause these to cancel and the correlation to disappear The level of digitisation will also depend on the type of experiment and the data one expects to extract from it. For absolute-value COSY, one is usually interested in establishing where correlations exist, with little interest in the fine structure within these crosspeaks. In this case, it is possible to use a low level of digitisation consistent with identifying correlations. As a rule of thumb, a digital resolution of J to 2J Hz/pt (AQ of 1/J to 1/2J s) should enable the detection of most correlations arising from couplings of J Hz or greater. Thus for a lower limit of, say, 3 Hz, a digital resolution of 3–6 Hz/pt (AQ of ~300– 150 ms) will suffice. The AQ_{t1} is typically half that for t_2 in this experiment, with one level of zero- filling applied in t1 so that the final digital resolution is the same in both dimensions of the spectrum (as required for symmetrisation).

For phase-sensitive data acquisitions, one is likely to be interested in using the information contained within the crosspeak multiplet structures, and a higher degree of digitisation is required to adequately reflect this, a more appropriate target being around J/2 Hz/pt or better (AQ of 2/J s or greater). Again, digitisation in t_2 is usually two or even four or eight times greater than that in t1. In either dimension, but most often in t_1, this may be improved

by zero-filling, although one must always remember that it is the length of the time-domain acquisition that places a fundamental limit on peak resolution and the effective linewidths after digitisation, regardless of zero-filling. The alternative approach for extending the time domain data is to use forward linear prediction when processing the data. The rule as ever is that high resolution requires long data-sampling periods.

Having decided on suitable digitisation levels and data sizes, one is left to choose the number of scans or transients to be collected per FID and the repetition rates and hence relaxation delays to employ. The minimum number of transients is dictated by the minimum number of steps in the phase cycle used to select the desired signals. Further scans may include additional steps in the cycle to suppress artefacts arising from imperfections. Beyond this, further transients should be required only for signal averaging when sensitivity becomes a limiting factor. Since most experiments are acquired under ‘steady-state’ conditions, it is also necessary to include ‘dummy’ scans prior to data acquisition to allow the steady state to establish. On modern instruments that utilize double buffering of the acquisition memory, dummy scans are required only at the very beginning of each experiment to make a negligible increase to the total time required. On older instruments that lack this feature, it is necessary to add dummy scans for each t_1

increment, and these may then make a significant contribution to the total duration of the experiment. The repetition rate will depend upon the proton T_1s in the molecule, and since the sequence uses 90^0 pulses, the optimum sensitivity is achieved by repeating every 1.3 T_1s.

Returning to the example of 400MHz acquisition discussed above, we can apply more appropriate criteria to the selection of parameters. Table 1 compares the result from above with more realistic data, and it is clear that under these conditions, COSY becomes a viable experiment, requiring only hours or even minutes to collect, rather than many days. The introduction of PFGs to high-resolution spectroscopy allows experiments to be acquired with only one transient per FID where sensitivity is not limiting, thus further reducing the total time required for data collection. The data storage requirements in these realistic examples are also well within the capabilities of modern computing hardware and are likely to become increasingly less significant as this develops further.

Table-1: Illustrative data tables for COSY experiments

Experiment	Spectral width/ppm	N(t_2)	N(t_1)	Hz/pt (t_2)	Hz/pt (t_1)	Experiment time	Raw data-set size
(a) Phase-sensitive	10 × 10	32K	32K	0.25	0.25	4.5 days	1000 M words
(b) Phase-sensitive	6 × 6	2K	1K	2.3	2.3	55 min	2 M words
(c) Absolute value	6 × 6	1K	256	4.6	4.6	22 min	0.25 M words

Scenario (a) transplants acquisition parameters from a typical 1D proton spectrum into the second dimension leading to unacceptable time requirements, whereas (b) and (c) use parameters more appropriate to 2D acquisitions. All calculations use phase cycles for f1 quad detection and axial-peak suppression only and for (b) and (c), a recovery delay of 1 s between scans. A single zero-filling in f1 was also employed for (b) and (c).

III. Results & Discussion

For the current study sample of Glimpride was taken for the analysis and than the data was interpreted using the correlation spectroscopy NMR technique. Proton NMR data was acquired in DMSO solvent and the result was found to be :- s(1H;10.38);t(1H;8.37);d(2H;7.81);d(2H;7.46);d(1H;6.36);s(2H;4.16);q(2H;3.52);q(1H;3.18); t(2H;2.89);q(2H;2.20);s(3H;2.01);m(4H;1.69);s(1H;1.24);q(2H;1.12);t(3H;1.10);t(2H;1.04); d(3H;0.95)

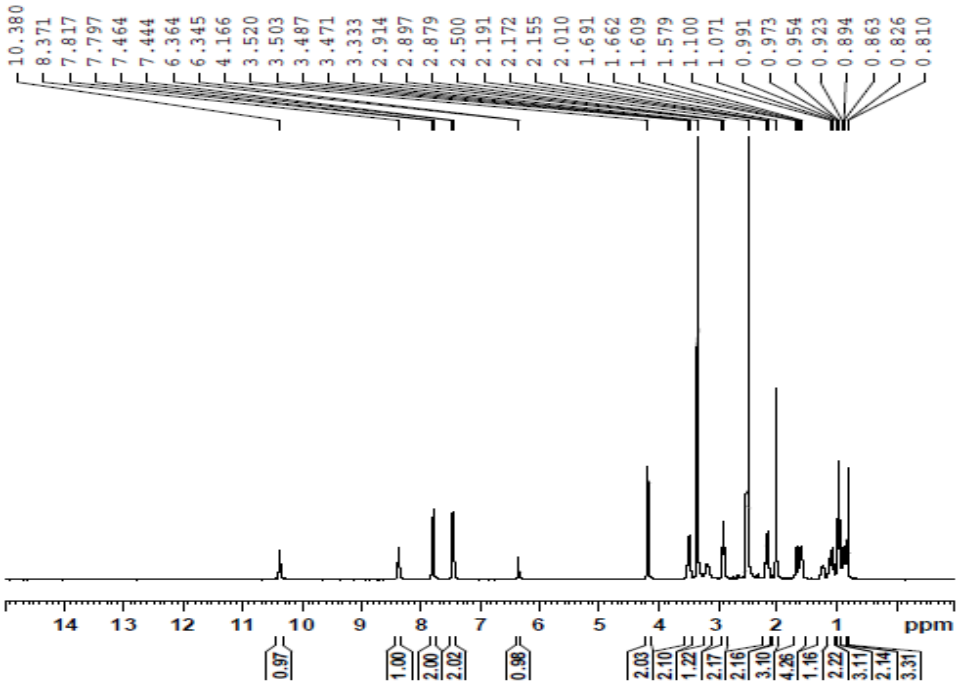

Figure-6:- Proton NMR Spectrum of Glimpride in DMSO (Bruker-400 MHz)

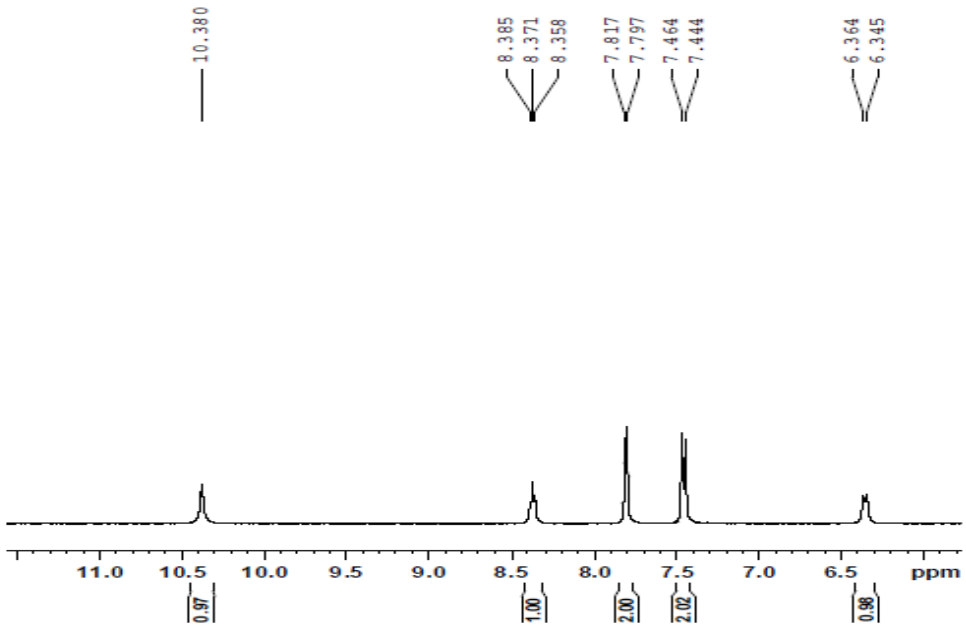

Figure-7:- Expanded view (aromatic region)of proton NMR Spectrum of Glimpride in DMSO (Bruker-400 MHz)

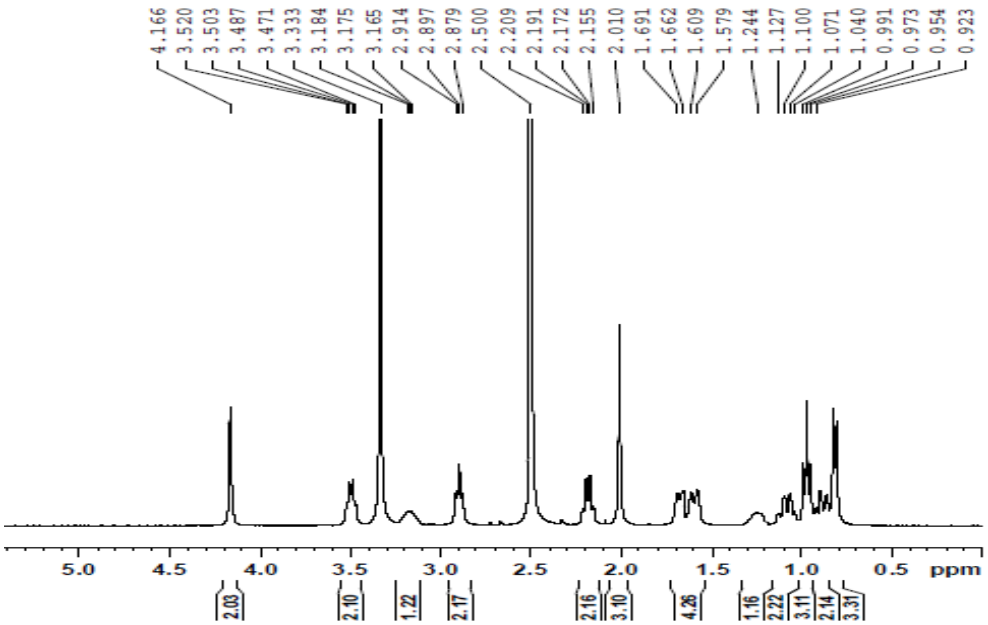

Figure-8:- Expanded view (aliphatic region)of proton NMR Spectrum of Glimpride in DMSO (Bruker-400 MHz)

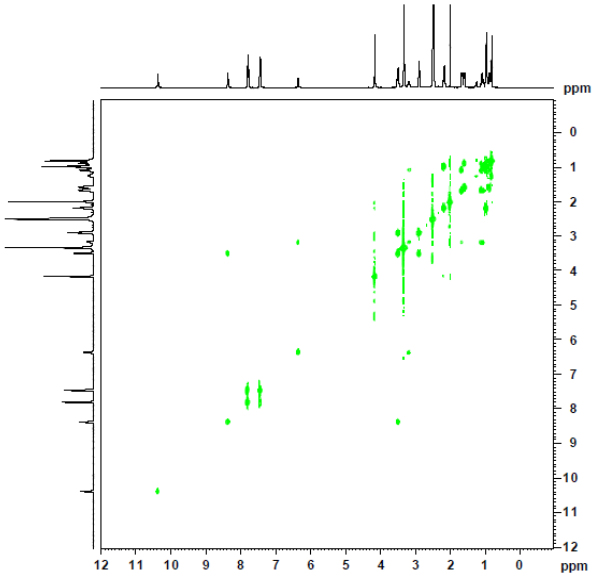

Figure-9:- COSY NMR Spectrum of Glimpride in DMSO (Bruker-400 MHz)

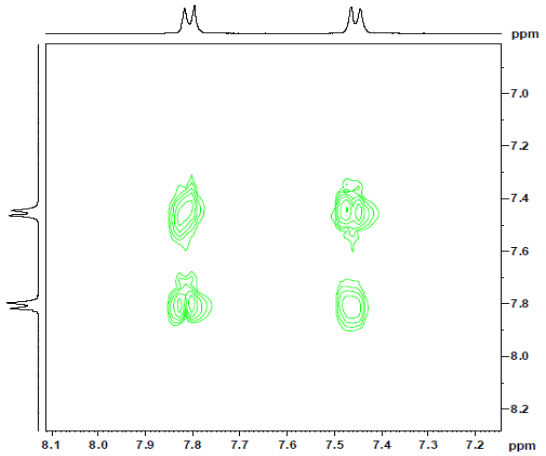

Figure-10:- Expanded view of COSY NMR Spectrum(aromatic region) of Glimpride in DMSO (Bruker-400 MHz)

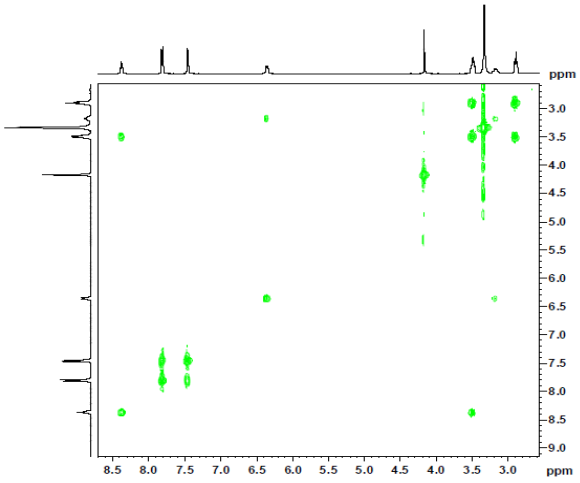

Figure-11:- Expanded view of COSY NMR Spectrum(aliphatic region) of Glimpride in DMSO (Bruker-400 MHz)

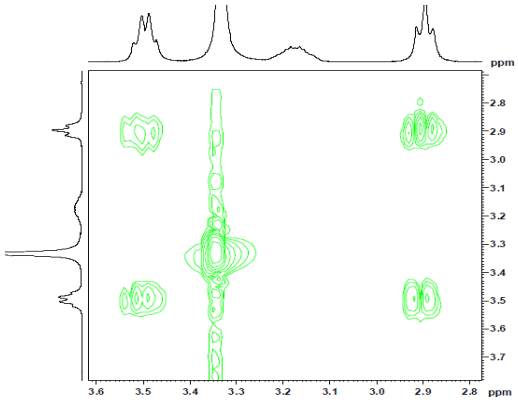

Figure-12:- Expanded view of COSY NMR Spectrum(aliphatic region) of Glimpride in DMSO (Bruker-400 MHz)

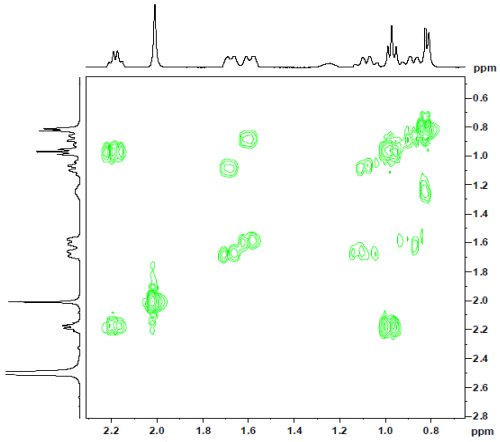

Figure-13:- Expanded view of COSY NMR Spectrum(aliphatic region) of Glimpride in DMSO (Bruker-400 MHz)

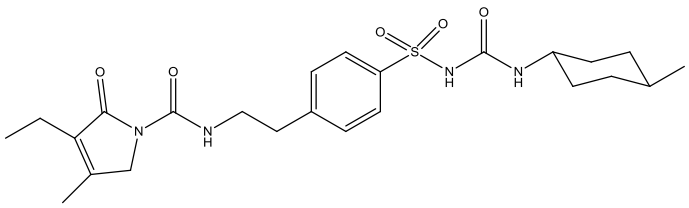

Figure-14:- Structure of glimpride

IUPAC name of glimpride: **3-ethyl-4-methyl-N-(4-(N-(((1r,4r)-4-methylcyclohexyl)carbamoyl)sulfamoyl)phenethyl)-2-oxo-2,5-dihydro-1H-pyrrole-1-carboxamide.**

From the spectral analysis we were able to deduce all the protons of the drug, the three protons coming at 10.38 ppm(1H;s);8.37ppm(1H;t);6.36ppm(1H;d) are for the NH protons j,e,k respectively

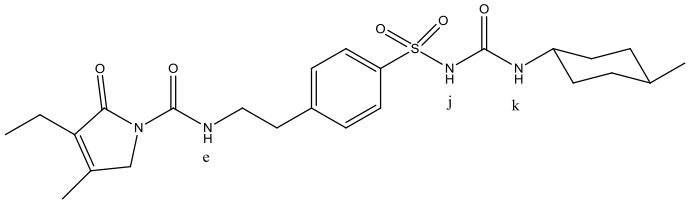

Figure-15:- Structure of glimpride showing NH protons.

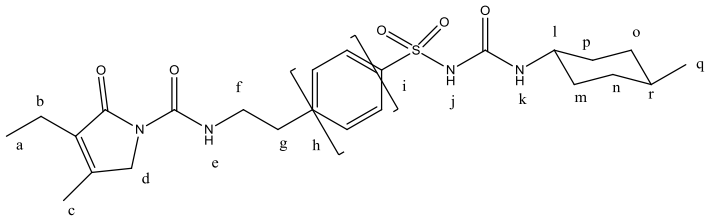

Figure-16:- Structure of glimpride showing labeling of all the protons.

From the analysis we were able to deduce that protons 'i' and 'h ' are coming as doublets at 7.81 ppm and 7.46 ppm respectively. There are three CH_3(methyl protons) 'a'; 'c' & 'q' which are coming as triplet(0.97 ppm), singlet (2.01ppm) and doublet(0.82ppm) respectively. Rest of the protons are provided as under:

S.No	Proton	Chemical Shift
1	b	2.17ppm
2	d	4.16ppm
3	f	3.49ppm
4	g	2.89ppm
5	l	3.17ppm
6	m	1.69ppm
7	n	1.10ppm
8	o	0.89ppm
9	p	1.60ppm
10	r	1.24ppm

Table 2: Table showing all the labeled protons value of Glimepride drug, rest protons value are provided in the above para.

REFERENCES

[1] J. Jeener, Ampe`re International Summer School, Basko Polje, (former) Yugoslavia, 1971.

[2] W. P. Aue, E. Bartholdi and R. R. Ernst, J. Chem. Phys., 1976, 64, 2229–2246.

[3] J. N. S. Evans, Biomolecular NMR Spectroscopy, Oxford University Press, Oxford, 1995.

[4] J. Cavanagh, W. J. Fairbrother, A. G. Palmer, N. J. Skelton and M. Rance, Protein NMR Spectroscopy:Principles and Practice, 2nd edition Academic Press (Elsevier), San Diego, 2006.

[5] J. Hahn, Higher-order 31P NMR spectroscopy of polyphosphorus compounds In: Phosphorus-31 NMR Spectroscopy in Stereochemical Analysis (Eds.: J.G. Verkade and L.D. Quin) VCH, Florida, 1987,pp. 331–364.

[6] D. J. States, R. A. Haberkorn and D. J. Ruben, J. Magn. Reson., 1982, 48, 286–292.

[7] M. Ohuchi, M. Hosono, K. Furihata and H. Seto, J. Magn. Reson., 1987, 72, 279–297.

[8] D. Marion and K. Wu¨thrich, Biochem. Biophys. Res. Commun., 1983, 113, 967–974.

[9] J. Keeler and D. Neuhaus, J. Magn. Reson., 1985, 63, 454–472.

[10] D. Marion, M. Ikura, R. Tschudin and A. Bax, J. Magn. Reson., 1989, 85, 393–399.